International Journal of Fracture **58**: 193–210, 1992.

Comparison between various displacement-based stress intensity factor computation techniques

I.L. LIM, I.W. JOHNSTON and S.K. CHOI*
Department of Civil Engineering, Monash University, Clayton, Victoria 3168, Australia;
**Division of Geomechanics, CSIRO, Syndal, Victoria 3149, Australia*

Received 25 August 1991; accepted in revised form 1 June 1992

Abstract. The computation of the stress intensity factor at a crack tip can be determined from the nodal displacements along the crack face. Amongst the existing techniques available are the Displacement Correlation Technique (DCT), the Quarter-Point Displacement Technique (QPDT) and the Displacement Extrapolation Technique (DET). As each of these techniques are popular in general LEFM analysis, an evaluation of their relative performances would seem appropriate. Previously, only limited comparisons have been made. In this paper the comparison is made on the basis of extensive numerical analysis. In addition two new variants to the DET are introduced and shown to be more efficient computationally.

The results indicate that the QPDT is generally more accurate and consistent in performance than the DCT. The DET, however, exhibited some erratic characteristics. Detailed examinations revealed that the linear regression analysis employed in the DET for the extrapolation is highly sensitive to the nodal displacement distribution. Both the new variant DETs exhibited much more consistent behaviour.

Nomenclatures

a = crack length
$e^{*i} = \dfrac{K^{*i} - K^{\text{exact}}}{K^{\text{exact}}}$
e^{DCT} = error in SIF computation associated with DCT
$e^{\text{QPDT}} = e^{*i}$, error in SIF computation associated with QPDT
G = shear modulus
K_{num} = numerically computed SIF
K_{anal} = analytical solution for SIF
K^{*i} = SIF computed from ith nodal pair along crack face
K^{XT} = SIF computed using X technique
L_N = size of normal element
L_Q = size of QPE element
L_S = size of singular element
L_T = size of transition element
N = number of K^{*i} in the set evaluated
r^{*i} = distance between ith node and the crack tip
u', v' = local displacement along and normal to crack axis
ρ = linear regression coefficient
υ = Poisson's ratio

1. Introduction

The finite element method has been employed extensively in fracture mechanics to model the stress singularity at the crack tip. In linear elastic fracture mechanics (LEFM) analysis, determination of the stress intensity factor (SIF) at the crack tip is often a major consideration and has to be evaluated as accurately as possible. A wide range of finite elements have been devised to achieve this. One approach is to utilise singular elements. Amongst those, the

quarter-point element (QPE) conceived by Barsoum [1] has found considerable popularity because of its simplicity and ease of implementation. In relation to the QPE, a number of SIF computation techniques have also been developed. The choice of the SIF computation technique is of importance as it should extract the best possible accuracy from a given deployment of singular elements.

In this study, only a number of displacement based methods will be examined. In particular, Displacement Correlation, Quarter Point Displacement and Displacement Extrapolation Techniques will be evaluated as they have been popular in general LEFM analysis. Their popularity stems from their ease of application and the reasonable accuracy possible. Although a number of comparative studies have been performed in the past on the above methods, they have usually been quite limited in scope. This study will examine the effect of QPE size variation on each SIF computation technique over a range of problems as well as the effect of employing transition elements. A number of variations to the Displacement Extrapolation Technique will also be proposed here.

2. SIF computation from QPE displacements

In this study, the following SIF computation techniques will be examined.

(a) *Displacement Correlation Technique (DCT)*
The SIF is easily computed using

$$K_{\mathrm{I}}^{\mathrm{DCT}} = \frac{G}{\kappa + 1}\sqrt{\frac{2\pi}{L_Q}}\{4(v'_B - v'_D) - (v'_C - v'_E)\},$$
$$K_{\mathrm{II}}^{\mathrm{DCT}} = \frac{G}{\kappa + 1}\sqrt{\frac{2\pi}{L_Q}}\{4(u'_B - u'_D) - (u'_C - u'_E)\}, \tag{1}$$

where G is the shear modulus, κ is $(3 - \upsilon)/(1 + \upsilon)$ for plane stress and also $3 - 4\upsilon$ for plane strain and axisymmetry, υ is the Poisson's ratio, L_Q is the length of QPE along crack face, and u', v' is the local displacement along and normal to crack axis as depicted in Fig. 1.

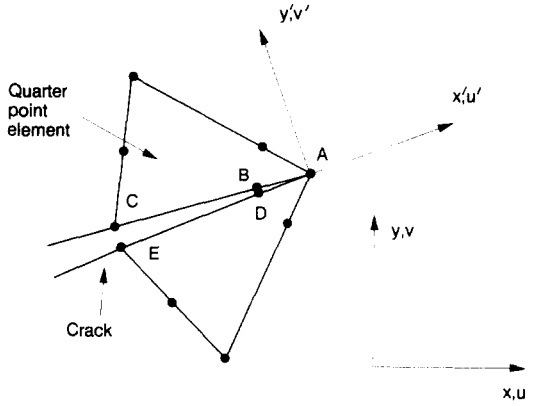

Fig. 1. Nodal lettering for stress intensity computations.

(b) *Quarter Point Displacement Technique (QPDT)*

The SIF is given by

$$K_{\mathrm{I}}^{\mathrm{QPDT}} = \frac{2G}{\kappa + 1}\sqrt{\frac{2\pi}{L_Q}}\{v'_B - v'_D\},$$
$$K_{\mathrm{II}}^{\mathrm{QPDT}} = \frac{2G}{\kappa + 1}\sqrt{\frac{2\pi}{L_Q}}\{u'_B - u'_D\}, \tag{2}$$

where all variables are as defined in (1).

Differing opinions presently exist regarding the preference of one method over the other. Traditionally, the DCT has been widely accepted to be the more accurate method. This was possibly initiated by Shih et al. [2] and Tracey [3] who both pointed out that the DCT is more rational in its formulation than the QPDT. This view was reinforced by limited numerical analyses performed by Shih et al. [2]. More recently, Yehia and Shephard [4] and Lim et al. [5] both reported that the QPDT is generally more accurate and less sensitive to the QPE size variation compared to the DCT. Their conclusions were based on a wider range of problems than that of Shih et al. [2]. An in-depth examination into the performances of both techniques was undertaken by Lim et al. [5]. They showed that the DCT was related to QPDT by

$$K^{\mathrm{DCT}} = 2K^{*1} - K^{*2}, \tag{3}$$

where K^{DCT} is the SIF computed according to DCT and K^{*i} is the SIF computed from the ith nodal pair using a similar form to (2). Hence $K^{*i} = K^{\mathrm{QPDT}}$.

This leads to

$$e^{\mathrm{DCT}} = 2e^{*1} - e^{*2}, \tag{4}$$

where e^{DCT} is the error in SIF computation associated with DCT, e^{*i} is $(K^{*i} - K^{\mathrm{exact}})/K^{\mathrm{exact}}$ and e^{*1} is equal to e^{QPDT}.

From the above, they showed that when the QPE size (L_Q) reduces to zero, $e^{\mathrm{DCT}} \to e^{\mathrm{QPDT}}$. However, as L_Q increases then in general $|e^{\mathrm{DCT}}| > |e^{\mathrm{QPDT}}|$, as (4) tends to amplify the errors for the DCT over that associated with the quarter-point node. Numerical results forwarded affirmed their arguments. However, their investigation did not consider the effect of employing transition elements [6]. This study will also examine this aspect.

3. SIF computation by extrapolation

(a) *Displacement Extrapolation Technique (DET)*

This technique was first employed by Chan et al. [7] who estimated the SIF by extrapolating the nodal displacements along the crack face. The expression is given as

$$K_{\mathrm{I}}^{\mathrm{DET}} = \lim_{r^{*i} \to 0} K_{\mathrm{I}}^{*i},$$
$$K_{\mathrm{II}}^{\mathrm{DET}} = \lim_{r^{*i} \to 0} K_{\mathrm{II}}^{*i}, \tag{5}$$

and

$$K_{\mathrm{I}}^{*i} = \frac{G}{\kappa + 1}\sqrt{\frac{2\pi}{r^{*i}}}\,v'(r^{*i}),$$
$$K_{\mathrm{II}}^{*i} = \frac{G}{\kappa + 1}\sqrt{\frac{2\pi}{r^{*i}}}\,u'(r^{*i}), \tag{6}$$

where r^{*i} is the distance between ith node and the crack tip.

The extrapolation was applied to the nodal K^{*i} along the crack face since along any other ray, additional terms to $r^{-1/2}$ must be considered [8] thereby rendering it more difficult and less accurate. Originally, the 'best' straight line was fitted empirically. This lack of consistency was addressed by Bank-Sills and Einav [9] who advocated the use of linear regression techniques. In essence, all possible sequential combinations of the nodal K^{*i} are evaluated. Figure 2 depicts some possible combinations. It is important to note that the K^{*i} associated with the quarter-point node is never included in the combinations because it has been found to provide unreliable SIF estimates when utilised in DET. With each combination set of the nodal K^{*i}, the linear correlation coefficient ρ is evaluated given that

$$\rho = \frac{\left(\Sigma x_i y_i - \frac{1}{N}\Sigma x_i y_i\right)}{\left\{\left[\Sigma x_i^2 - \frac{1}{N}(\Sigma x_i)^2\right]\left[\Sigma y_i^2 - \frac{1}{N}(\Sigma y_i)^2\right]\right\}^{1/2}}, \tag{7}$$

where x_i is equal to r^{*i}, y_i is equal to K^{*i} and N is the number of K^{*i} in the set evaluated.

The 'best' straight line is one which produces a value of ρ closest to unity. Its corresponding intercept with the ordinate at $r = 0$ is K^{DET}. In such an approach, $0.5(N-1)(N-2)$ combination sets must be evaluated. Consequently, the DET requires a substantially increased computa-

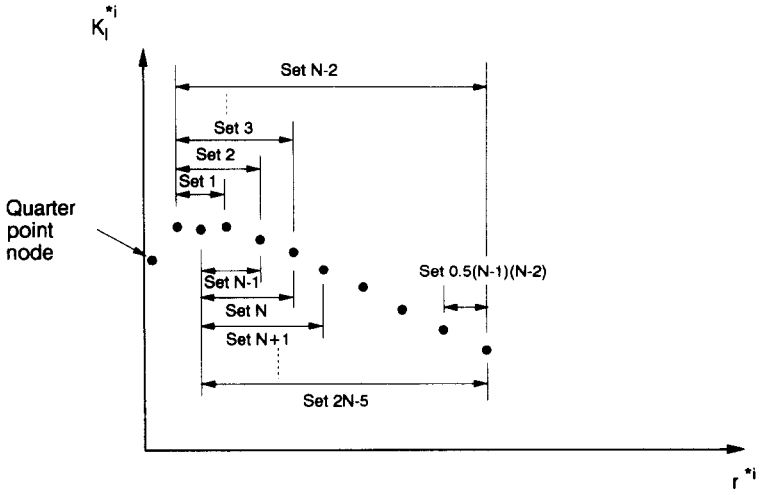

Fig. 2. Sequential combinations of K^{*i} are evaluated using linear regression.

tional effort in SIF estimation as compared to either DCT or QPDT. However, Bank-Sills and Einav [9] advocated the use of the DET as it appeared to provide more accurate results than the DCT.

A major shortcoming in this method is its implicit assumption that the nodal K^{*i} should vary linearly along the crack face. Carpenter [10] proved analytically that the displacements (and stresses) along any ray emanating from the crack tip generally do not vary linearly. However, for the case of the single edge crack configuration under uniform tension, it was demonstrated that the displacements do vary linearly along the crack face. This explains the excellent results procured by Chan et al. [7] for this configuration. In analyses involving discrete crack propagation, this weakness may well be exacerbated. For such analyses usually involve complex interactions between the cracked body and applied tractions. The possibility of obtaining a linear variation in displacements along the crack face may be expected to be extremely remote.

Another possible difficulty is envisaged in partial crack closure problems as depicted in Fig. 3. If the extrapolation was applied to section A where the crack face is separated, it would differ greatly from that obtained from section B. It is likely that any lack of linearity in the displacements along the crack face will be accentuated in such situations.

(b) *Reduced Displacement Extrapolation Technique (RDET)*

As the DET requires a much greater computational effort than the DCT or QDPT, it may be desirable to improve its efficiency. This may be achieved by restricting the possible sequential combinations of the nodal K^{*i} to start only at a given node. It is proposed here that a suitable starting node is the QPE corner node. This node is closest to the crack tip after the quarter-point node. The quarter point itself was not considered because it has proved to be unsuitable for use with such extrapolation techniques [9]. The use of the next closest node was chosen to ensure that the possible combinations of the nodal K^{*i} adequately reflect the SIF at the crack tip. However, it does not completely overcome the shortcomings associated with DET.

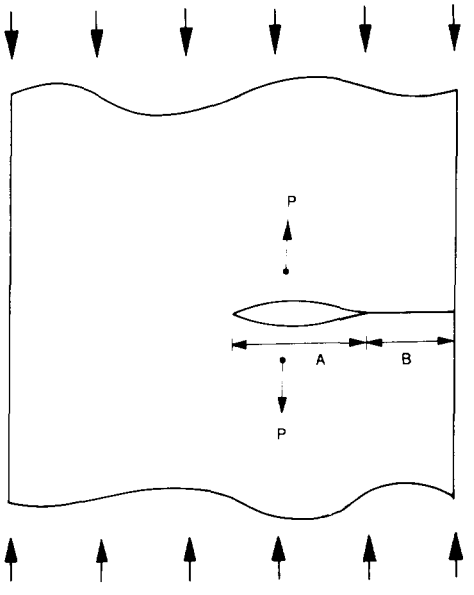

Fig. 3. A partial crack closure problem.

For the set consisting of a combination of nodal K^{*i} may still include nodes far removed from the crack tip where the assumption of linearity in the nodal K^{*i} may be inappropriate for the displacements associated with such a wide range of nodes. However, its computational effort is reduced to only $(N-2)$ evaluations.

(c) *Limited Displacement Extrapolation Technique (LDET)*
Another variant to the DET is to apply further restrictions to the possible combinations of K^{*i}. It is proposed that only three nodal K^{*i} values associated with an element immediately adjacent to the QPE be utilised. Mathematically, it means

$$K^{\mathrm{LDET}} = \lim_{r^{*i} \to 0} F(K^{*2}, K^{*3}, K^{*4}), \tag{8}$$

where F is a 'best' fitted line through K^{*2}, K^{*3} and K^{*4} and i ranges from 2 to 4. This technique requires only one linear regression analysis, thereby reducing the computational effort considerably.

This approach does not eliminate all shortcomings associated with DET. However, it does substantially reduce the possibility of being affected by those shortcomings. For example, if the element from which K^{LDET} is computed is small and located very near the crack tip, it is reasonable to assume that any non-linear displacement variation in the crack tip vicinity may be adequately represented by a linear function. In partial crack closure problems, the possibility of K^{LDET} representing the actual SIF is enhanced considerably as it is unlikely that any of the three nodes would lie in a section which is not representative of the crack tip SIF. On the other hand, this method is now much more sensitive to the local variation in displacements near the crack tip. The performance of all the proposed variants in displacement extrapolation techniques will be examined in this study.

4. Numerical analyses

Three test problems of increasing complexity were selected. The first is the centre cracked panel (CCP) under uniform tension [11]. Second is the standard ASTM three point bend (TPB) specimen [12]. Last is the inclined single edge crack (ISE) subjected to a uniform bending moment [13]. Mixed-mode conditions apply to the ISE configuration. Both the CCP and TPB problems are of practical significance in fracture testing whereas the ISE was chosen to provide indications of performance for more general problems. In order to concentrate solely on the effect of QPE and transition element size variations, attempts were made to eliminate other possible influencing factors. In all crack configurations as depicted in Fig. 4, the finite element mesh was delineated into an outer and inner (shaded) mesh. The outer mesh was kept unchanged while all variations occurred within the inner mesh. The only mesh parameters modified were the number of element layers, the element type and their relative sizes. By so doing, the variation in SIF is dependent solely on changes within the inner mesh.

The optimal shape and arrangement identified by Lim et al. [14] were employed. Eight equilateral triangular QPEs were arranged symmetrically in a rosette around the crack tip. Other additional layers of transition and/or normal elements may be placed symmetrically surrounding the QPE rosette. The outer-most element layer within the inner mesh always

consisted of normal elements designated as 'buffer' elements. Double precision was utilised for all nodal co-ordinates and for the finite element analyses. Attention to such details was made to minimise all possible sources of SIF computation error. Three point Gauss integration was employed for the QPE (consisting of natural isoparametric triangle elements) and all other triangular elements. The remaining elements were isoparametric quadrilateral elements. Analyses were made, employing both exact (9 Gauss) and reduced (4 Gauss) integration, but only the

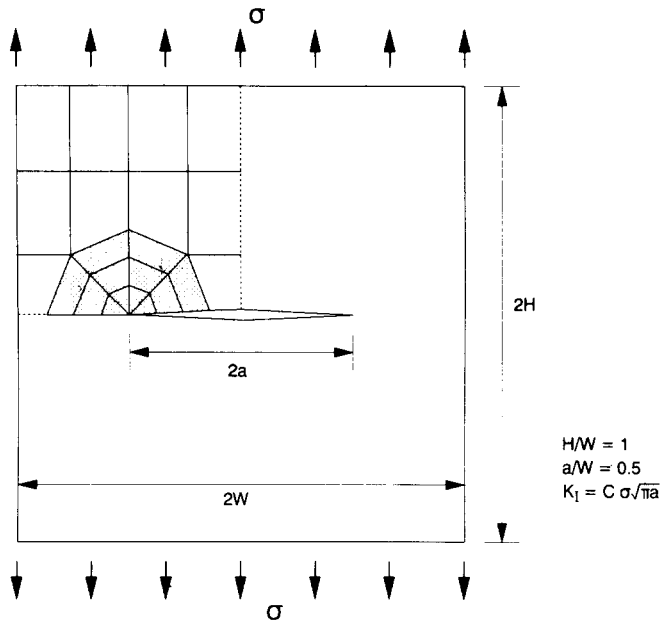

Fig. 4(a). Centre cracked panel under uniform tension.

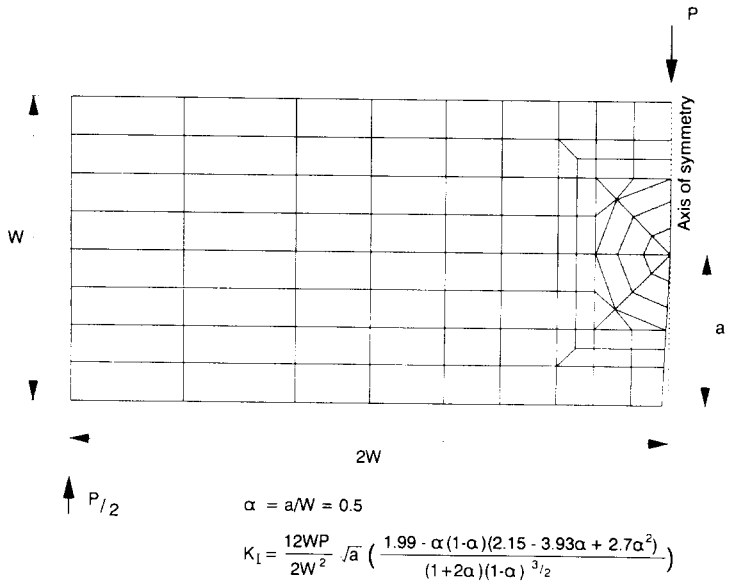

Fig. 4(b). Three point bend specimen.

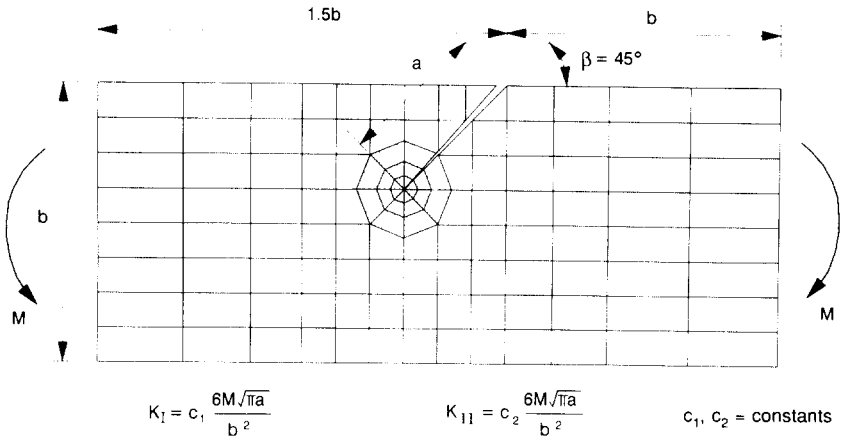

Fig. 4(c). Inclined single edge cracked configuration subjected to uniform bending moment.

results for the former will be presented here for reasons of brevity. It should be noted, however, that essentially similar characteristics were observed between the two integration orders. The only major difference was a slightly larger spread of errors evident for the analyses using reduced integration.

The analytical expressions for the SIF are provided in Fig. 4. The percentage errors as used in this study are defined as

$$\frac{K_{\text{num}} - K_{\text{anal}}}{K_{\text{anal}}} \times 100\% \tag{9}$$

where K_{num} is the computed SIF and K_{anal} is the analytical solution for SIF.

Over 500 analyses were performed. However, not all results are depicted in the figures presented in this study to avoid unnecessary congestion. Others were omitted simply because they lie beyond the specific area of interest. The trends and characteristics are presented by employing 'error curves' that link sets of results together.

5. Effect of the QPE size

The first set of analyses examined the effect of QPE size (L_Q) variation on the performance of the various SIF computation techniques. No transition elements were employed. Therefore, the inner mesh is now composed only of the QPE surrounded by a layer of buffer elements. In Fig. 5, it is obvious that the QPDT generally performs better than the DCT. In the comparison between the LDET and RDET, both appear to provide very similar results. The only exception is for ISE (mode I) where the RDET gave slightly better results compared to the LDET, as shown in Fig. 5(c).

In the comparison between the QPDT and the LDET or RDET, no clear conclusions can be made. For the case of the CCP problem as depicted in Fig. 5(a), the QPDT appears comparable in performance to either the LDET or RDET. However, for the ISE (mode II) configuration, the QPDT is clearly superior in performance (Fig. 5(d)). On the other hand, the LDET and RDET provided better results for the TPB problem as depicted in Fig. 5(b). Both techniques appeared

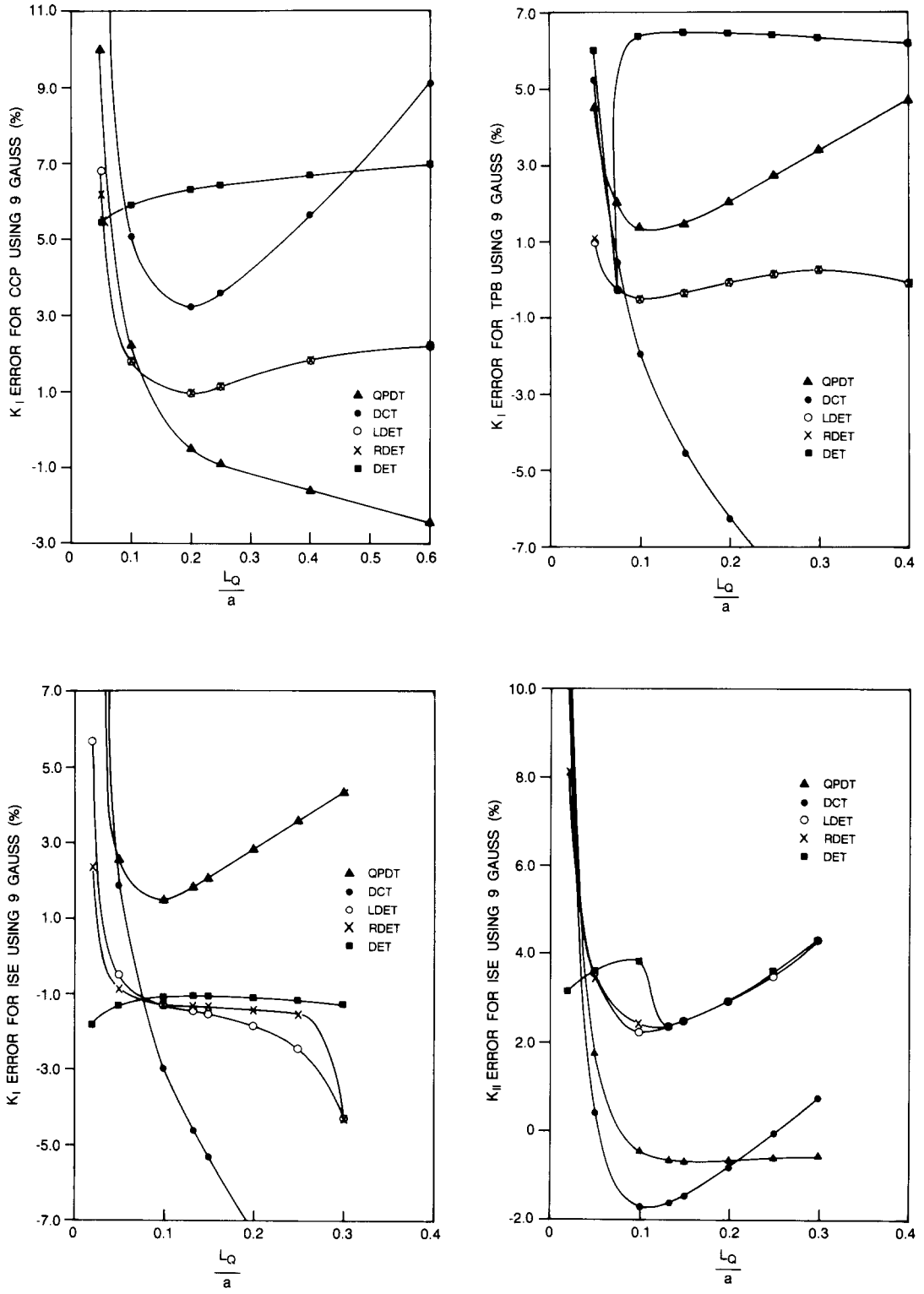

Fig. 5. Effect of QPE size on SIF error for various SIF computation techniques. (a) Centre cracked panel, (b) Three point bend, (c) Inclined single edge crack (mode I) and (d) Inclined single edge crack (mode II).

to be much less sensitive to the QPE size variation in contrast to the QPDT. In the case of the ISE (mode I) configuration, both LDET and RDET performed better when L_Q/a is small. With increasing L_Q, the QPDT soon performed comparably with either the LDET or RDET. It can only be concluded here that none of the three techniques are clearly superior to the other in terms of their performance.

The DET appears to perform in a distinctly different manner in comparison with the other methods. In the ISE (mode I) problem, the DET provides the best SIF estimation compared to the other methods as seen from Fig. 5(c). It also appears to be quite insensitive to the QPE size. For the ISE (mode II) given in Fig. 5(d), it performs adequately although there appears to be a kink in its result around $L_Q/a = 0.1$. However, for the CCP configuration (Fig. 5(a)) its estimation is the worst amongst the techniques examined here. Its error is at least 5 percent. A similar pattern emerges for the TPB problem. In addition, an obvious aberration occurs at $L_Q/a = 0.05$ as depicted in Fig. 5(b). The reason for such irregularities will be discussed at length in a later section.

6. Use of transition elements

A second series of analyses was performed to study the effect of using transition elements on the performance of the SIF computation techniques. A wide range of transition element sizes (L_T) was examined, including several sizes of normal elements (L_N). The results from the first set of analyses were included for comparative purposes. They were distinguished from the rest as having 'no transition elements'. Typical results are depicted in Fig. 6 for the TPB problem. In

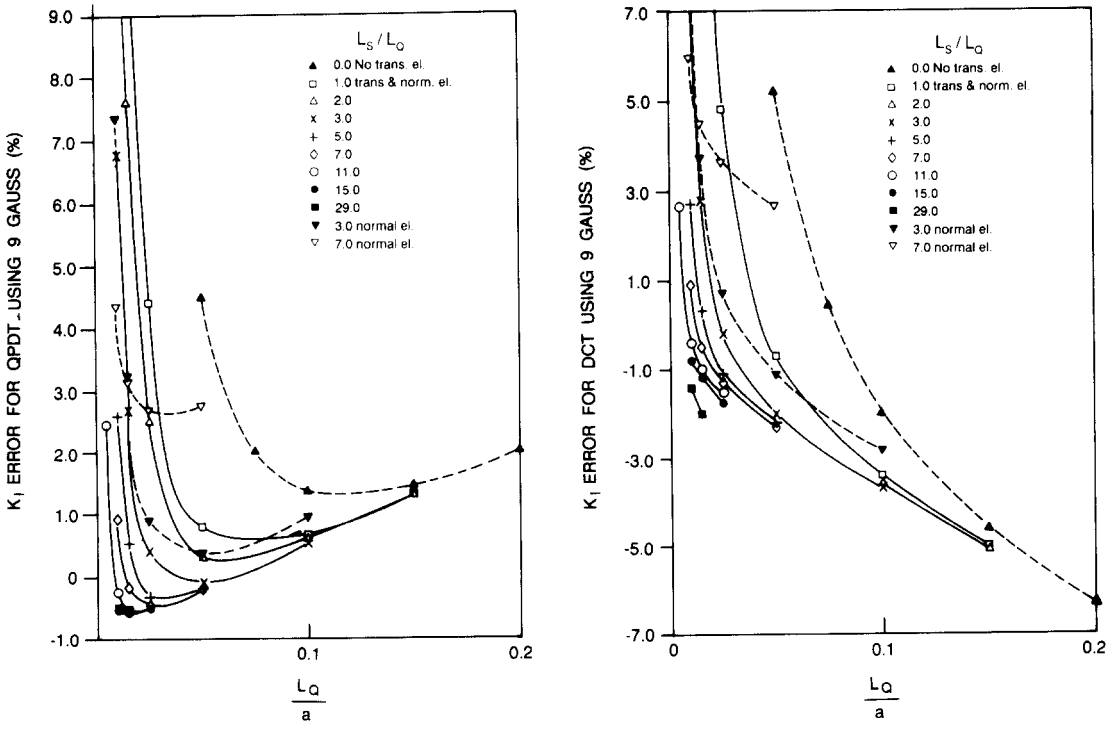

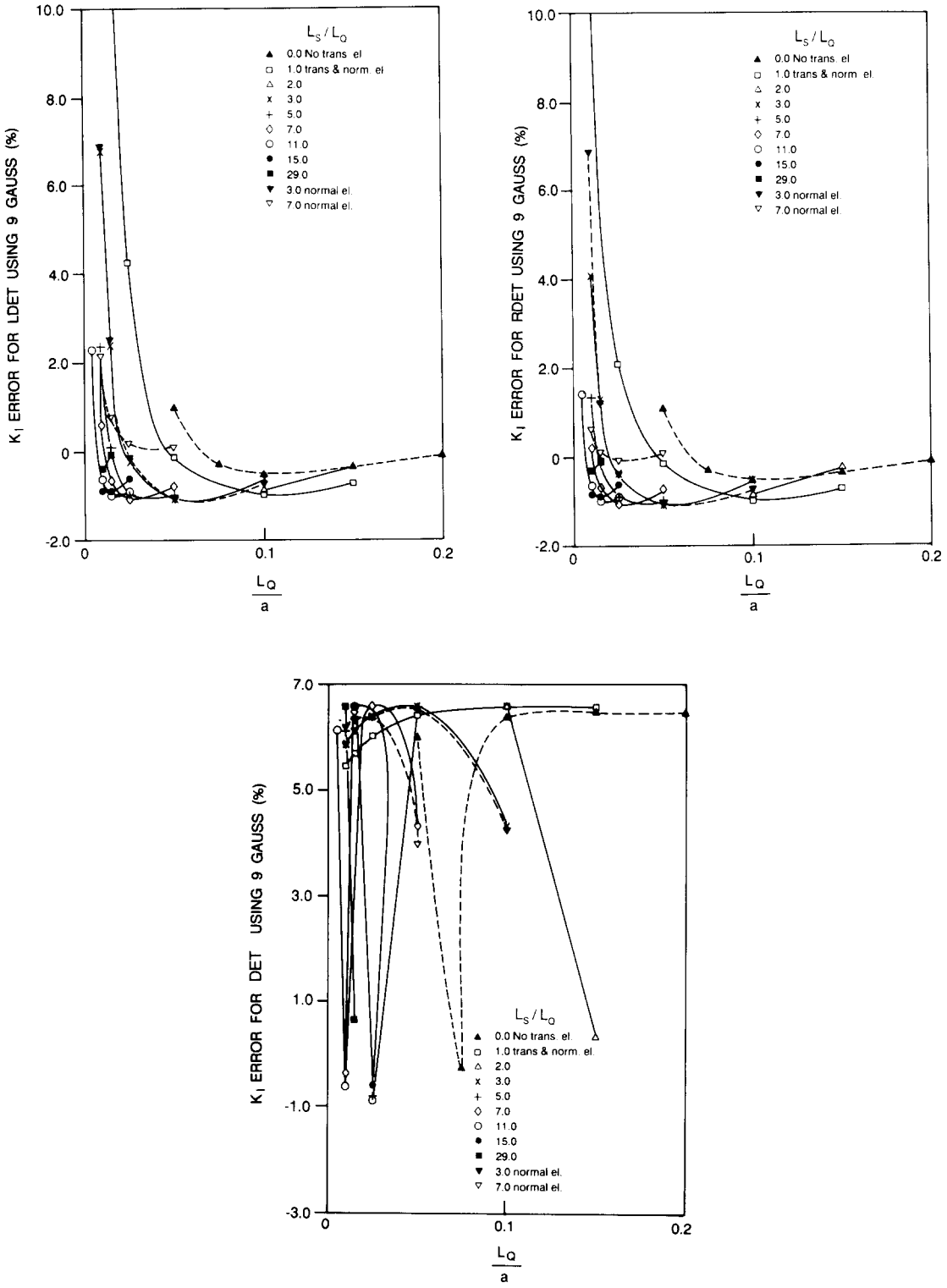

Fig. 6. Effect of various $L_S L_Q$ ratios on the SIF error for the three point bend problem using the (a) QPDT, (b) DCT, (c) LDET, (d) RDET, (e) DET.

Fig. 6, L_S is defined to be L_T or L_N (size of the normal elements immediately surrounding the QPE) as the case may be. For the most part, L_S represents the length of transition element used. When normal elements were employed in place of transition elements, it is noted in the figure. It is obvious from Fig. 6 that no optimal transition size exists regardless of the SIF computation technique employed.

The results were then replotted with $(L_S + L_Q)/a$ as the abscissa as shown in Fig. 7. In effect $(L_S + L_Q) = L_{SRZ}$ which is the Singularity Representation Zone (SRZ) size proposed by Lim et al. [14]. The SRZ is utilised to indicate whether adequate singularity modelling capability is being provided by the elements in that zone. The results in Fig. 7 now show clear trends in behaviour. Hence it confirms the importance of correctly defining and applying the SRZ concept. This concept appears to be valid regardless of the SIF computation techniques utilised here.

It is also noted that the results for $L_T/L_Q = 1$ and $L_N/L_Q = 1$ are almost identical regardless of the SIF computation technique employed. For that reason, this pair of results are combined together and represented as $L_S/L_Q = 1$ in Fig. 7. This provides further affirmation to Lim et al.'s [14] observation that normal elements behave similarly to transition elements when $L_T/L_Q = L_N/L_Q = 1$.

The overall behaviour corresponding to each technique is shown in Fig. 8 for each of the three problems. A number of observations may be made:

1. The DCT appears to exhibit the largest spread of error in SIF estimation as well as the worst accuracy, with the possible exception of the DET. The DCT consistently performs poorer than the QPDT. This lends weight to Lim et al.'s [5] argument that $|e^{DCT}| > |e^{QPDT}|$ in general.

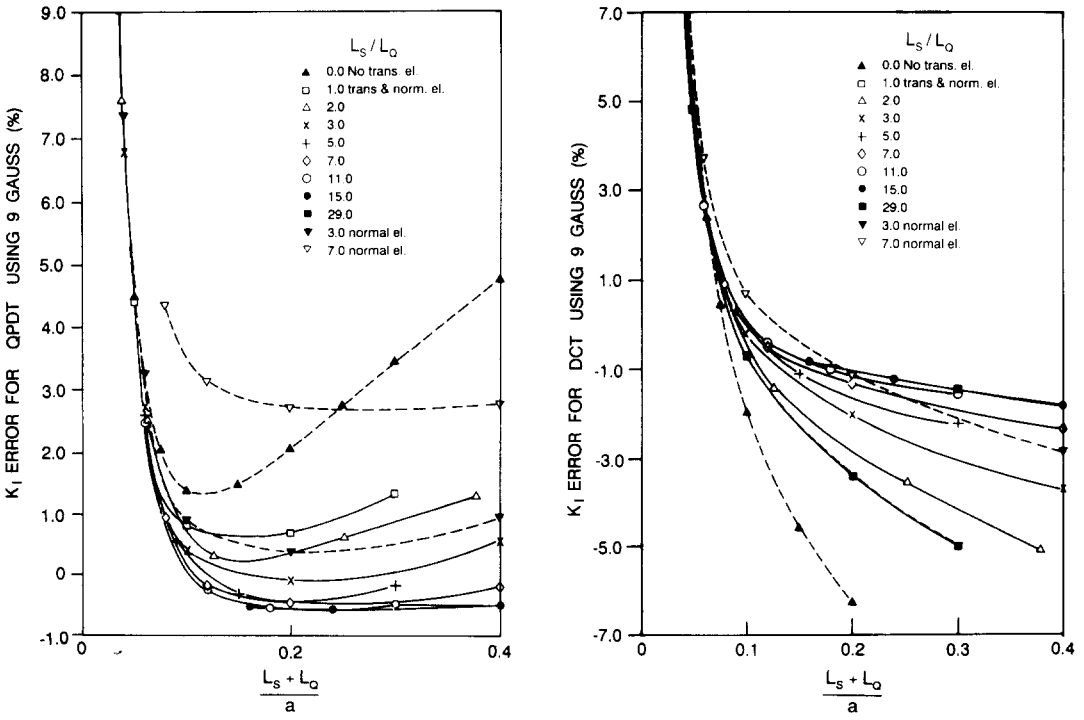

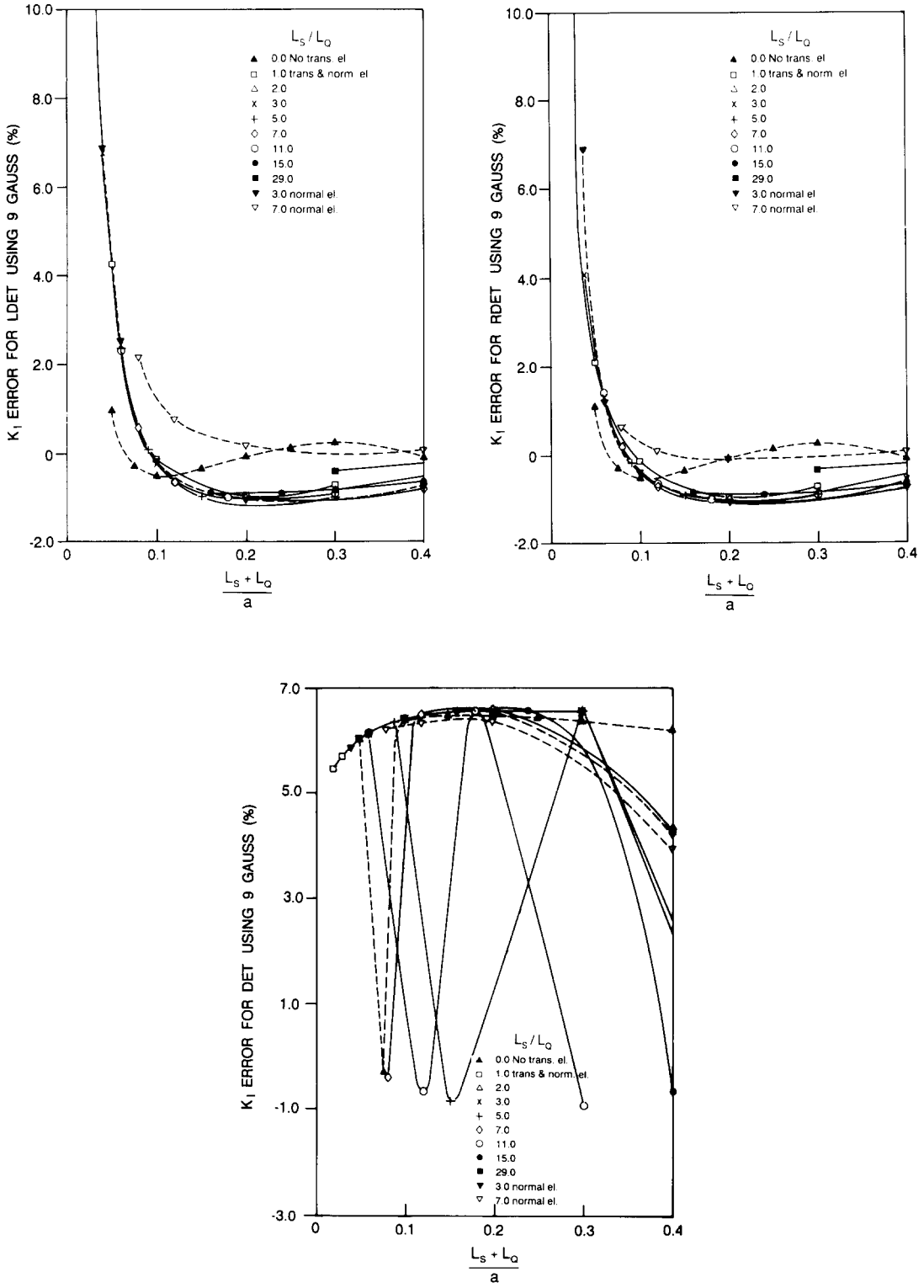

Fig. 7. Redefinition of Fig. 6 using the Singularity Representation Zone for the three point bend problem. (a) QPDT, (b) DCT, (c) LDET, (d) RDET, (e) DET.

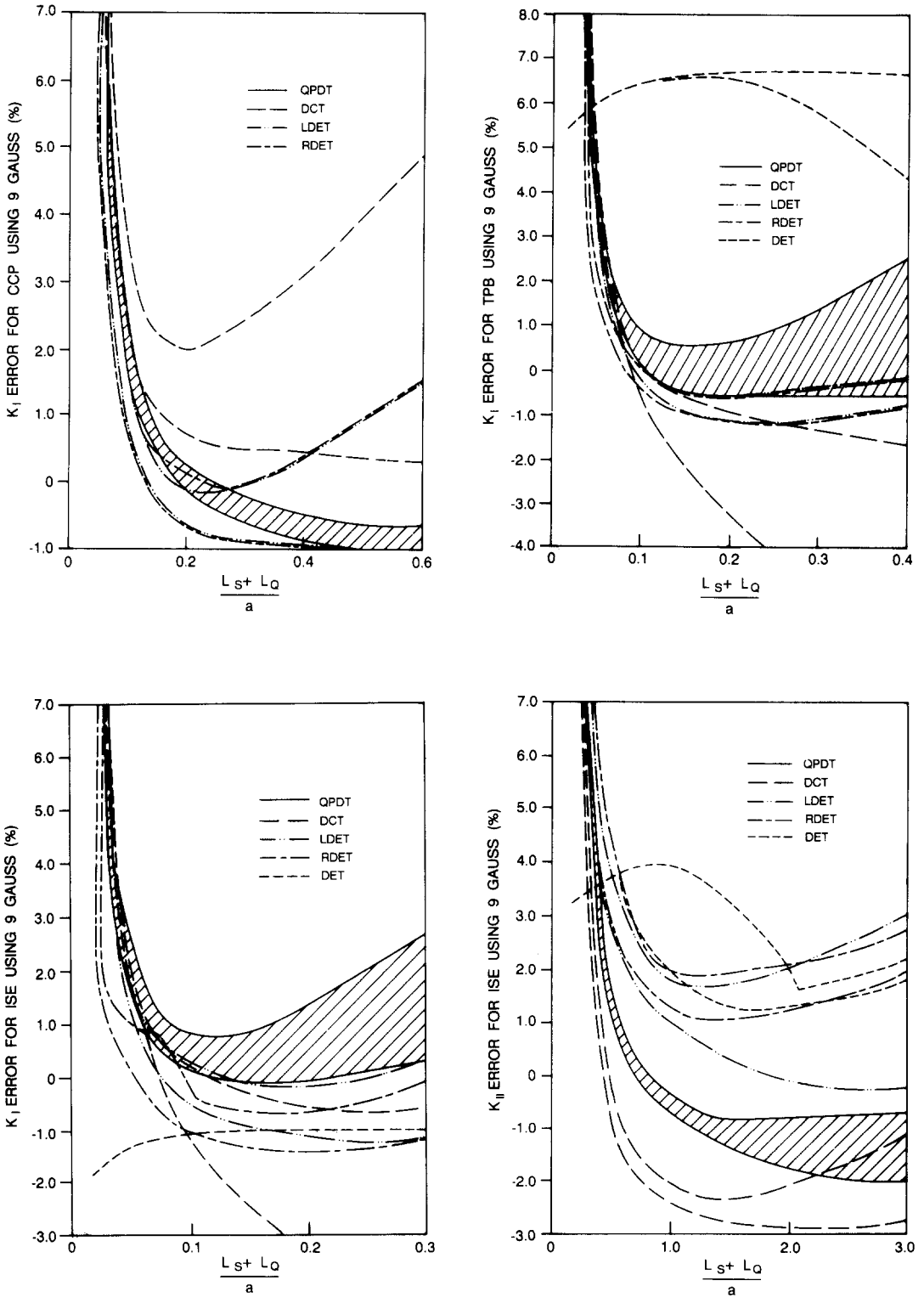

Fig. 8. A comparison between various SIF computation techniques for the (a) Centre cracked panel, (b) Three point bend, (c) Inclined single edge crack (mode I), (d) Inclined single edge crack (mode II).

2. The QPDT appears to perform well in general. Its performance seems to be comparable to that of RDET and LDET. It provides a better range of SIF for the CCP and ISE (mode II) than either RDET or LDET. However, the reverse is true for the remaining problems. When adequate SRZ size is used, it would appear that the QPDT can estimate the SIF well within ± 2 percent even though the meshes used were quite coarse.
3. The DET seems to behave in a totally different manner from the other techniques. It is obvious from Fig. 7(e) that there appears to be some irregularities in its performance. An in-depth examination of this anomaly will be conducted in the following section.
4. Generally, the LDET performs as well as the QPDT. In addition, it does not appear to exhibit any irregularities unlike the DET.
5. The RDET appears to perform similarly to the LDET in general. For the CCP and TPB problems, its behaviour almost mirrors that of the LDET. On the other hand, it shows a definite departure in performance for the ISE configuration. Some minor irregularities in the error curve pattern is evident in Fig. 8(c). Presumably this is because the RDET still has some of the characteristics associated with the DET.
6. While the use of transition elements generally tends to improve the results, it does not significantly alter the essential performance characteristic associated with the various techniques.

7. In-depth examination of extrapolation techniques

It is clearly evident in the previous section that some irregularities exist in the DET performance. To better understand this anomaly, a more detailed scrutiny of the results are necessary. For the purposes of this discussion, the results pertaining to the ISE (mode II) problem as shown in Fig. 9 is investigated. In Fig. 9, an obvious kink in the error curves at approximately $(L_S + L_Q)/a = 0.1$ is observed. Now, the variation of K along the crack face at various L_Q/a when $L_T/L_Q = 3$ is depicted in Fig. 10(a). Table 1 lists the variation of ρ for particular combination sets of the nodal K^{*i} corresponding to Fig. 10(a). In Table 1, it may be observed that there does not appear to be any clear relationship between ρ and L_Q/a. In fact, the value of ρ appears to fluctuate as L_Q/a increases. From (7), it would seem that ρ is a complicated function of the nodal location along the crack face as well as the nodal K^{*i} variation along the crack face. It is therefore not surprising that ρ may have no direct relationship with L_Q/a. For the most part, the combination set (6, 8) which represents the set of K^{*6} to K^{*8} inclusive, is used for the best fit line. However, at $L_Q/a = 0.05$, the combination set (3, 5) is chosen instead as it has a higher value of ρ. This abrupt switch in choice of combination sets resulted in a sudden dip in the error curve as seen in Fig. 9. Similar characteristics may also be observed in Fig. 10(b) and Table 2 where normal elements were employed in place of transition elements. Therefore this irregularity in the DET occurs regardless of the element type utilised. A close inspection of other configurations revealed similar characteristics. As an example, the erratic behaviour observed in Fig. 6(e) is explained by the selection of a particular combination set over another as L_Q/a is varied. When L_Q/a is small, combination set J is chosen over L. As L_Q/a is increased slightly, combination set L is now preferred over J as its ρ is the most optimum. With further increase in L_Q/a, combination set J is again chosen over L because its ρ is now the most optimum. The switching between the various combination sets results in erratic error curves.

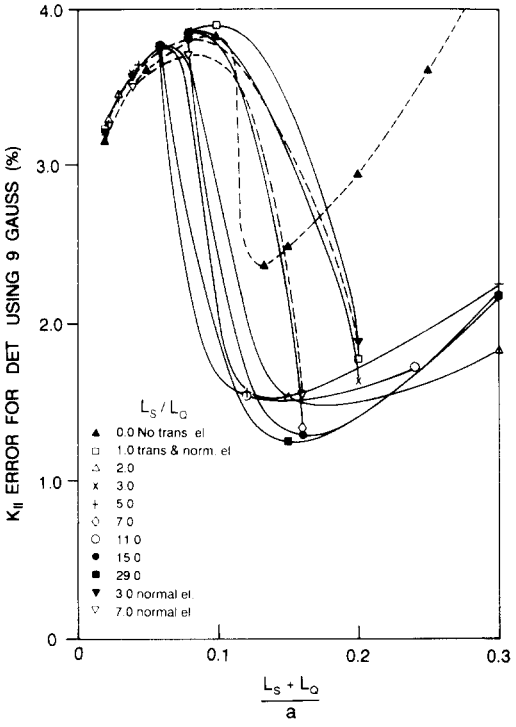

Fig. 9. Detailed result for the inclined single edge problem (mode II) using the DET.

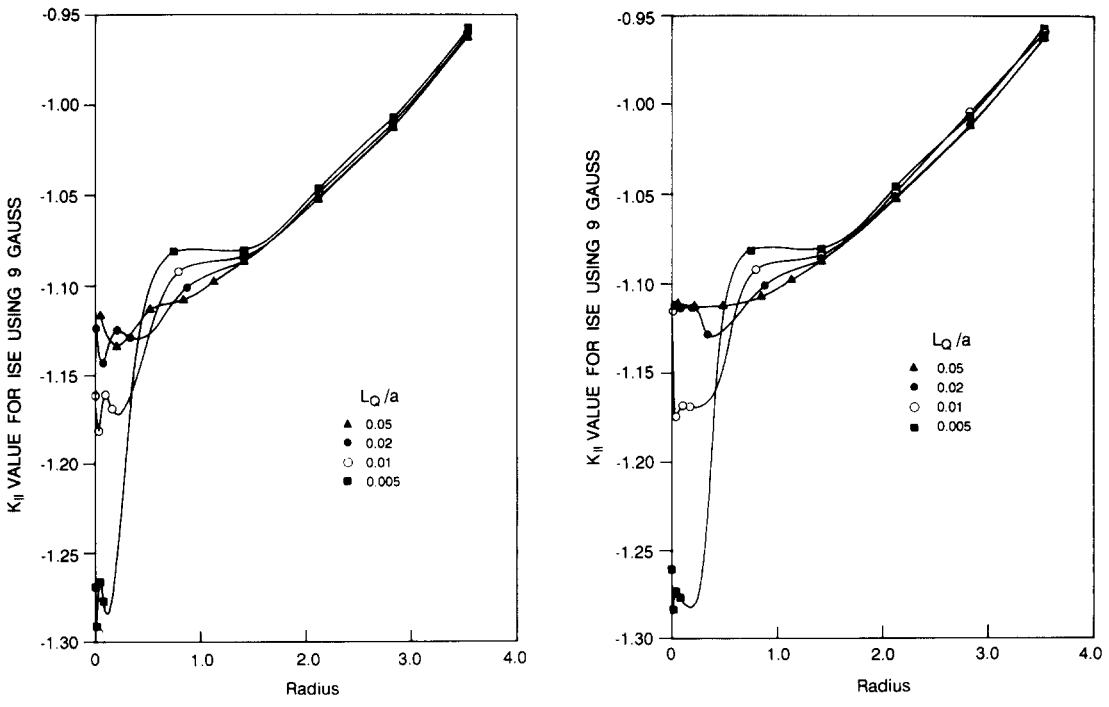

Fig. 10. Variation of K^{*i} along the crack face for the inclined single edge crack problem (mode II) when utilising (a) transition elements, (b) normal elements only.

Table 1. Effect of QPE size on the linear regression coefficient and the selected stress intensity factor when transition elements were employed

	$(3, 5)^+$		$(6, 8)^+$		Best fit	
L_Q/a	ρ	K^{DET}	ρ	K^{DET}	(a, b)	K^{DET}
0.005	0.99603	−12.94	0.99860	−11.55	(6, 8)	−11.55
0.001	0.98841	−11.83	0.99865	−11.59	(6, 8)	−11.59
0.02	0.98410	−11.41	0.99864	−11.62	(6, 8)	−11.62
0.05	0.99973	−11.37	0.99853	−11.62	(3, 5)	−11.37

$^+$ (a, b) means the combination set includes K^{*a} to K^{*b}

Table 2. Effect of QPE size on the linear regression coefficient and the selected stress intensity factor when transition elements were not employed

	$(4, 6)^+$		$(6, 8)^+$		Best fit	
L_Q/a	ρ	K^{DET}	ρ	K^{DET}	(a, b)	K^{DET}
0.005	0.75450	−12.57	0.99858	−11.55	(6, 8)	−11.55
0.01	0.82735	−11.69	0.99862	−11.59	(6, 8)	−11.59
0.02	0.96954	−11.40	0.99859	−11.61	(6, 8)	−11.61
0.05	0.99952	−11.40	0.99851	−11.62	(4, 6)	−11.40

$^+$ (a, b) means the combination set includes K^{*a} to K^{*b}

In the case of the LDET, only the combination set (3, 5) is evaluated. Consequently, the irregularity associated with DET is removed. However, for the RDET, occasional switching between combination sets may still occur.

From this study, it may be concluded that the DET should be used with care because of its erratic characteristics. This characteristic may be significantly reduced if the mesh is fine at the crack tip and the element size varies gradually away from the tip. Nevertheless, one cannot be completely assured that this erratic characteristic will be eliminated. It should be noted that Chan et al. [17] and Bank-Sills and Einav [9] did not report any aberrations in the use of the DET. However, they investigated simple mode I problems under uniform tension. In addition, fine meshes were employed at the crack tip with a gradual progression of element sizes away from the crack tip.

8. Conclusions

It was found that the QPDT generally performs better than the DCT. It was also shown that the DET may produce erratic performance because of its sensitivity to both the distribution of nodes along the crack face and the variation of K at each node. Amongst the two variants to the DET proposed in this study, the LDET avoids totally this erratic behavour.

Overall, both the QPDT and LDET performed equally well and were superior to the other methods studied. The QPDT might be given preference as it is the easiest to implement and the most efficient computationally.

Acknowledgment

This study forms part of the first author's Ph.D. thesis under the supervision of the other authors. The financial support provided by the Monash Graduate Scholarship is gratefully acknowledged.

References

1. R.S. Barsoum, *International Journal of Fracture* 10 (1974) RCR 603–605.
2. D.M. Tracey, *International Journal of Numerical Methods in Engineering* 11 (1977) 401–402.
3. C.F. Shih, H.G. de Lorenzi and M.D. German, *International Journal of Fracture* 12 (1976) RCR 647–651.
4. N.A.B. Yehia and M.S. Shephard, *International Journal of Numerical Methods in Engineering* 21 (1985) 1911–1924.
5. I.L. Lim, I.W. Johnston and S.K. Choi, *Communications in Applied Numerical Methods* 8 (1992) 291–300.
6. P.P. Lynn and A.R. Ingraffea, *International Journal of Numerical Methods in Engineering* 12 (1978) 1031–1036.
7. S.K. Chan, I.S. Tuba and W.K. Wilson, *Engineering Fracture Mechanics* 2 (1970) 1–17.
8. L. Bank-Sills and D. Sherman, *International Journal of Fracture* 32 (1986) 127–140.
9. L. Bank-Sills and O. Einav, *Computers and Structures* 25 (1987) 445–449.
10. W.C. Carpenter, *Engineering Fracture Mechanics* 18 (1983) 325–332.
11. M. Isida, *International Journal of Fracture* 7 (1971) 301–316.
12. J.E. Srawley, *International Journal of Fracture* 12 (1976) RCR 475–476.
13. W.K. Wilson, Research Report *69-1E7-FMECH-R1*, Westinghouse Research Laboratories, Pittsburgh (1969).
14. I.L. Lim, I.W. Johnston and S.K. Choi, *International Journal of Numerical Methods in Engineering* (1991) submitted.